Direct Determination of the Hole Density of States in Undoped and Doped Amorphous Organic Films with High Lateral Resolution

O. Tal,[1,*] Y. Rosenwaks,[1,†] Y. Preezant,[2] N. Tessler,[2] C. K. Chan,[3] and A. Kahn[3]

[1]*Department of Physical Electronics, Tel Aviv University, Tel Aviv 69978, Israel*

[2]*Department of Electrical Engineering, Technion Israel institute of Technology, Haifa 32000, Israel*

[3]*Department of Electrical Engineering, Princeton University, Princeton, New Jersey 08544, USA*

(Received 21 August 2005; published 16 December 2005)

We investigate the density of states (DOS) for hole transport in undoped and doped amorphous organic films using high lateral resolution Kelvin probe force microscopy. Measurements are done on field effect transistors made of *N, N*$^{\mathrm{I}}$-diphenyl-*N*, *N*$^{\mathrm{I}}$-bis(1-naphthyl)-1,10-biphenyl–4,4$^{\mathrm{II}}$-diamine undoped or *p* doped with tetrafluoro-tetracyanoquinodimethane. We determine the DOS structure of the undoped material, including an anomalous peak related to interfaces between regions of different surface potential, the DOS doping-induced broadening, and doping-induced sharp peaks on the main DOS distribution.

DOI: 10.1103/PhysRevLett.95.256405 PACS numbers: 71.23.−k, 73.20.At, 73.50.−h, 73.61.−r

The density of states (DOS) for charge-carrier transport in organic molecular films and the impact of electrical doping on the DOS are of fundamental importance for understanding charge transport in organic films. Transport in amorphous organic semiconductors is generally described in terms of charge-carrier hopping between disordered localized energy states [1]. The energy disorder is ascribed to the different environment of each molecule: Static and dynamic disorder in position and orientation affect the molecular energy levels through electrostatic [2,3] and steric [4] interactions. This disorder leads to a DOS usually modeled by a Gaussian [2] or exponential [5] distribution. The insertion of dopant molecules, i.e., electron donors or acceptors or optical dopants, further modifies this DOS. Dopants are introduced either intentionally, to improve the film conductivity [6], modify charge injection barriers [7], add functionality (e.g., a *pn* junction [8]), and modify the film optical properties [9], or unintentionally, as synthesis impurities [10], solution residuals [11], and chemically induced doping [12], which deteriorate the performance of the organic material. In any case, an accurate understanding of the DOS energy distribution and how it is affected by molecular doping is one of the keys to advancing basic research on, and technological applications of, organic semiconductor films, since many electronic properties of organic semiconductors are closely related to the shape of the DOS [13,14].

The influence of dopants on the DOS distribution has been studied indirectly by assuming a Gaussian DOS distribution and extracting function parameters from carrier mobility measurements as a function of doping concentration. It was found that the DOS distribution broadens with increasing doping concentration [6], a tendency that was attributed to potential fluctuations caused by the Coulomb field of the randomly distributed dopant [15,16]. However, experimental information on the specific shape of the DOS relevant to carrier transport in organic films has been very limited, and the influence of doping on the DOS has never been explored directly. Lang *et al.* have used current-voltage measurements as a function of temperature in organic thin film transistors (OTFTs) to extract the density of gap states in amorphous and single crystal pentacene [17], and Hulea *et al.* have used an electrochemically gated transistor to measure a wide energy range of the highest occupied molecular orbital (HOMO) DOS in poly(*p*-phenylenevinilene) by injection of holes and ionized dopants in different concentrations during the measurement [18].

In this Letter, we report the direct determination of the DOS around the HOMO level in undoped and doped amorphous organic thin films using Kelvin probe force microscopy (KPFM) measurements on an OTFT structure. We observe a broadening of the DOS distribution, as well as sharp doping-induced peaks in the DOS distribution. Exploiting the KPFM nanoscale lateral resolution, an additional peak is observed in the main DOS distribution of the undoped film at specific sites located at interfaces between regions of different surface potential, while the doped films exhibit a laterally more homogeneous DOS distribution.

The OTFT structure (Fig. 1) consisted of a heavily doped *p*-type silicon gate electrode, a thermally grown 90 nm silicon oxide gate insulator, and 50 nm thick gold strips evaporated on the oxide to form source and drain electrodes separated by 16 μm. A thin film (10 nm) of *N, N*$^{\mathrm{I}}$-diphenyl-*N*, *N*$^{\mathrm{I}}$-bis(1-naphthyl)-1,10-biphenyl–4,4$^{\mathrm{II}}$-diamine (α-NPD) was deposited on the substrate by sublimation in an ultrahigh vacuum chamber. Doped α-NPD films were formed by coevaporation of tetrafluoro-tetracyano-quinodimethane (F_4-TCNQ) with the host molecules [19]. The transistors were transported under nitrogen atmosphere to a nitrogen glove box (<2 ppm H_2O) in which the KPFM (Autoprobe CP—Veeco Inc. with homemade Kelvin probe electronics) is located. A semiconductor parameter analyzer (HP 4155C) was used

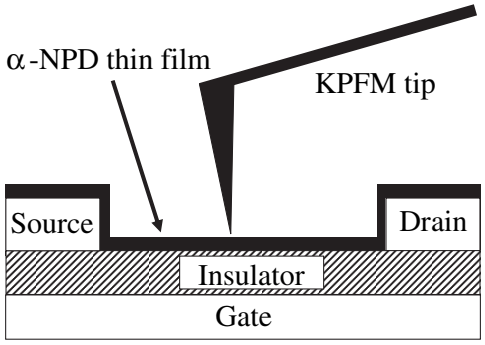

FIG. 1. Schematic of the OFET structure and KPFM tip above the channel.

to control the gate voltage, with respect to the grounded source and drain electrodes, and monitor the drain, source, and gate electrode currents. The contact resistance [20,21], leakage current through the gate insulator and to the periphery of the active area, and shifts of the threshold voltage [20] due to continuous voltage application were found to be negligible in these transistor structures.

The OFETs were scanned with the KPFM across relatively smooth regions of the organic layer (roughness $<$ 1 nm) at different gate potentials. When the gate-source voltage (V_{GS}) is lower than the threshold voltage (V_t), which is defined as the V_{GS} at flat levels condition [22] or zero level shift in thin enough organic films, holes are injected into the organic film and populate the edge states of the HOMO, and the molecular energy levels shift toward the chemical potential (μ) energy level. During the measurement, μ is kept constant by grounding the source and drain contacts, and the molecular energy levels are shifted with respect to μ by the gate-induced voltage.

According to numerical calculations [23] conducted for a 10 nm thick organic layer in an OFET structure and different Gaussian DOS distributions, the induced charge is approximately homogeneously distributed across the organic film width, and the energy level bending from the film surface to the film/gate-insulator interface is negligible for the measured V_{GS} range. We emphasize that this assumption holds up only to a certain V_{GS}; according to our calculations, above this V_{GS} [24], the conducting channel is squeezed toward the gate insulator and the level bending is not negligible. This behavior has already been reported elsewhere [22,25]. Under a negligible level bending condition, the shift of the energy levels (V_L) for different V_{GS} with respect to the level position at $V_{GS} = V_t$ can be measured directly by the KPFM: $V_L(x) = \mathrm{CPD}(x) - \mathrm{CPD}_t(x)$, where CPD($x$) is the contact potential difference measured between the KPFM tip and the sample at a given location (x) across the transistor, and $\mathrm{CPD}_t(x)$ is measured at $V_{GS} = V_t$. The DOS is then calculated using

$$g(qV_L(x)) = (C_{ox}/d_{org}q^2)[(dV_L(x)/d(V_{GS} - V_t))^{-1} - 1], \quad (1)$$

where C_{ox} is the silicon oxide capacitance per unit area, d_{org} is the organic film thickness and q is the electron charge.

The inset in Fig. 2(a) shows the V_L measured across an undoped transistor. The potential of the grounded source and drain appears as the flat portion at each end of the curves, and the potential distribution across the organic channel is seen in between. The curves were measured for $V_{DS} = 0$ V and V_{GS} ranging from 0 to -16.5 V. Figure 2(a) shows V_L measured as described in the inset across the organic film far from the drain and source electrodes, as a function of $V_{GS} - V_t$ [26] for undoped (curve A) and doped α-NPD (curve B). The doping concentration is $1.4(\pm 0.4) \times 10^{18}$ cm^{-3} ($\sim 0.1\%$ of the total molecular density) [27]. Each curve is an average of 50 curves measured at different locations on the transistors to reduce the experimental uncertainty. Measurements on different transistors gave very similar results. The curves for both undoped and doped layers show that the change in V_L is largest at small $|V_{GS}|$, then decreases, and finally saturates as $|V_{GS}|$ increases. During this process, the

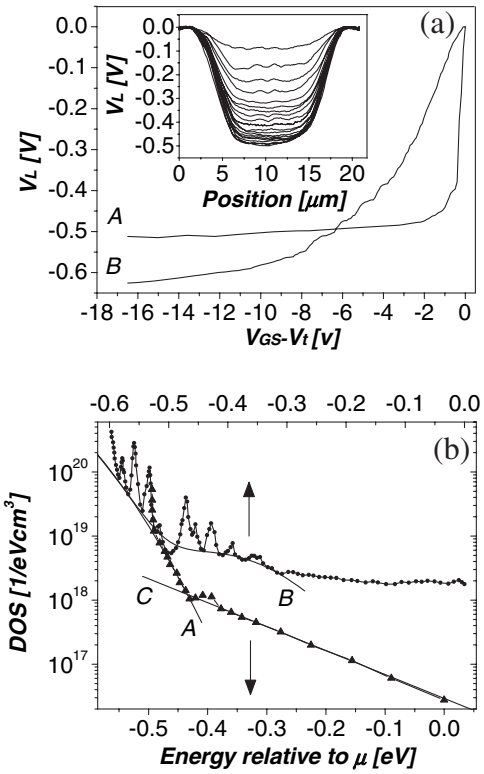

FIG. 2. (a) Inset: V_L profiles measured across an undoped transistor for $V_{DS} = 0$ V and V_{GS} ranging from 0 to -16.5 V. (a) V_L as a function of $V_{GS} - V_t$ measured on undoped (A) and doped (B) samples. (b) DOS vs energy relative to μ for $V_{GS} = V_t$ for undoped (solid triangles) and doped (solid circles) samples. The solid curves are a fitting of a Gaussian function [Eq. (2); curve A] and an exponential function [Eq. (4); curve B] to given ranges in the undoped sample DOS curve and a fitting of Eq. (3) (curve C) to the doped sample DOS curve.

HOMO shifts toward μ and holes are injected into available states near μ. A low state density results in a larger change in V_L and vice versa; hence, the slope of the $V_L/(V_{GS} - V_t)$ curve is inversely proportional to the DOS. It points to an increase in the DOS as μ penetrates deeper into the HOMO state distribution, while the fine structure observed on the curves is a result of finer changes in the DOS. The V_L saturation at large enough $|V_{GS}|$ possibly stems from the onset of large level bending near the gate insulator at high charge concentrations or from μ pinning at high DOS.

The DOS vs qV_L in Fig. 2(b) is obtained for undoped (triangles) and doped (circles) samples by applying Eq. (1) to the data of Fig. 2(a). The energy scale in Fig. 2(b) represents the energy relative to μ for $V_{GS} = V_t$, and the negative sign denotes values below μ. The sharp increase in DOS near the high-energy end of the curves [left side of Fig. 2(b)] should be considered as a measurement artifact that reflects the termination of the level shift [V_L saturation as appears in Fig. 2(a)]. While the DOS of the undoped sample has a single peak around 0.408 ± 0.005 eV in the measured energy range, the DOS of the doped sample exhibits several peaks at (0.356, 0.393, 0.431, 0.456, 0.472, 0.518, 0.534, 0.560, 0.850) $\pm$ 0.005 eV. These peaks imply the presence of several doping-induced energy levels. A variety of dopant configurations, i.e., dopant clusters with various sizes or different configurations of dopant and host molecules, can lead to local shifts in potential energy and result in several discrete energy levels, as is measured here.

The DOS in the undoped sample can be divided into three main regions: a tail, a single peak around $E = 0.408 \pm 0.005$ eV, and a region that can be fitted to a Gaussian distribution [13] [curve A in Fig. 2(b)]:

$$g_i(E) = [N_i/(\sigma\sqrt{2\pi})]\exp[-((E - E_c)/(\sqrt{2}\sigma))^2]. \quad (2)$$

Inserting the total state density $N_i = 1.2 \times 10^{21}$ cm^{-3} for α-NPD (equivalent to one state per molecule), we find a Gaussian width (variance) $\sigma = 0.10 \pm 0.01$ eV centered at $E_c = -0.84 \pm 0.04$ eV. This width should be considered with care, since the Gaussian function is fitted to a relatively small range of the measured DOS curve; however, it can serve as a guiding parameter that can be applied to an analytical expression that describes the influence of doping on the DOS [15]:

$$g(E) = [(N_i - N_a)/N_i]g_i(E) + [N_a/N_i]g_i(E + e^2/(4\pi\varepsilon\varepsilon_0 a) - \sqrt{e^3F/(\pi\varepsilon\varepsilon_0)}), \quad (3)$$

where $g_i(E)$ is given by Eq. (2), $N_a = 1.4(\pm 0.4) \times 10^{18}$ cm^{-3} is the doping concentration, $a = 0.6$ nm is the distance between a dopant and the nearest intrinsic hopping site [15], ε_0 is the dielectric permittivity, $\varepsilon = 3$ is the relative dielectric constant of α-NPD [19], and $E_c = -0.88 \pm 0.04$ eV [appeared in $g_i(E)$, Eq. (2)], which is in good agreement with the E_c of curve A. The lateral electric field (F) between the source and the drain is considered equal to zero since the drain-source voltage is zero. Equation (3) yields the curve B in Fig. 2(b) and describes well the main DOS distribution of the doped sample. According to Ref. [15], the second term in Eq. (3) expresses the shift of states toward the center of the gap due to the presence of dopants; note that its contribution in curve B is observed mostly at $E \geq -0.49$ eV. Further examination of the measured DOS of the undoped sample reveals a DOS tail at $-0.38 \leq E \leq 0$ eV that can be fitted to an exponential function [5] [curve C in Fig. 2(b)]:

$$g(E) = [N_t/(kT_0)]\exp[-E/(kT_0)], \quad (4)$$

with a total trap density $N_t = 3.4 \times 10^{15}$ cm^{-3} and an effective temperature $T_0 = 1350$ K. In the case of the doped sample, a moderately sloped exponential-like DOS tail, which deviates from curve C, appears at $-0.31 \leq E \leq 0$ eV. The observed flattening and rising of the exponential tail due to doping has been previously described with an analytical model for an exponential DOS tail [28]. The described changes point to a DOS broadening due to doping, as was also observed indirectly by other methods [6].

KPFM topographic measurements across various transistor regions show a smooth organic film surface, yet concomitant CPD measurements show randomly distributed potential fluctuations in both doped and undoped samples. The inset in Fig. 3(a) shows such fluctuations in V_L profile measured across the central region of an undoped transistor channel at $V_{GS} = -0.1$ V. The DOS presented in Fig. 3(a) is measured at the center of the potential depressions and protrusions (locations a, c, and e in the inset) and at their interfaces (location b, d, and f). An additional peak appears at $E = 0.408 \pm 0.05$ eV on the main DOS distribution measured at these interfaces. A possible origin for this additional intensity in the state distribution is the presence of interface states between molecular aggregates with slightly different averaged molecular orientation, leading to differences in the measured CPD. For the doped sample, DOS distributions measured at five different locations [Fig. 3(b)] show the same distribution of the main peaks with different amplitudes. The additional peak seen in the DOS of the undoped film [Fig. 3(a)] may be masked by the dopant-induced changes in the DOS of the doped film. The average lateral separation between the dopants is around 10 nm; this is less than the KPFM spatial resolution, estimated to be tens of nanometers; thus, DOS fluctuations in the vicinity of a specific dopant are most likely not detected, and the different peak amplitudes at different locations may stem from changes in the relative contributions of the various dopant energies.

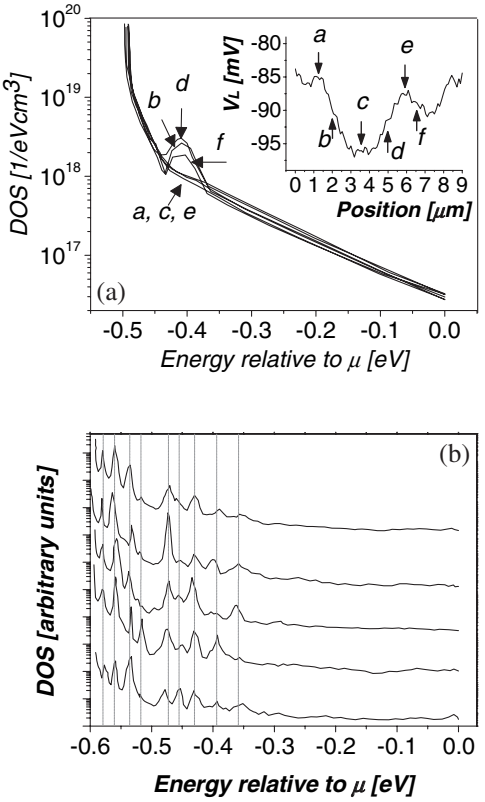

FIG. 3. (a) Inset: V_L profile measured across the channel of an undoped transistor. (a) DOS distributions measured at different lateral locations across the channel marked as a–f in the inset. (b) DOS distributions measured at different lateral locations across the channel of doped transistor. Each DOS curve is an average of three curves that were measured at the same location.

In conclusion, the KPFM-based method described here allows the direct determination of the DOS distribution in a molecular film and of the influence of doping on this distribution, with a lateral resolution of tens of nanometers. The DOS of the undoped organic film exhibits an exponential-like tail and a more complex structure, including an additional peak at specific physical locations on the film that correspond to interfaces between regions with different surface potential. Doping broadens the DOS and induces several discrete peaks on the main distribution. DOS distributions measured at different lateral positions on the doped samples have similar shape and peak energies but different peak heights. Such sensitive DOS measurements provide new information on the effect of doping on the electronic energy states distribution. This information is crucial for understanding carrier transport in amorphous organic semiconductors.

This research was generously supported by the U.S.–Israel Binational Science Foundation (BSF), Grant No. 2000-092. The authors thank J. Klafter for fruitful discussions. A. K. also gratefully acknowledges partial support of the work by the NSF (DMR-0408589).

*Electronic address: orent@eng.tau.ac.il
†Electronic address: yossir@eng.tau.ac.il

[1] H. Bassler, Phys. Status Solidi B **175**, 15 (1993).
[2] S. V. Novikov *et al.*, Phys. Rev. Lett. **81**, 4472 (1998).
[3] S. V. Novikov, Phys. Status Solidi B **236**, 119 (2003).
[4] Z. G. Yu *et al.*, Phys. Rev. B **63**, 085202 (2001).
[5] M. C. J. M. Vissenberg and M. Matters, Phys. Rev. B **57**, 12 964 (1998).
[6] Y. Shen *et al.*, Phys. Rev. B **68**, 081204(R) (2003).
[7] M. Gross *et al.*, Nature (London) **405**, 661 (2000).
[8] P. Qibing *et al.*, Science **269**, 1086 (1995).
[9] S. Welter, L. Brunner, J. W. Hofstraat, and L. De Cola, Nature (London) **421**, 54 (2003).
[10] S. Naka *et al.*, Synth. Met. **111**, 331 (2000).
[11] K. Sakai and K. Ikezaki, in *Proceedings of the 11th International Symposium on Electrets (ISE11), Melbourne, Australia, 2002* (IEEE, Piscataway, NJ, 2002), p. 151.
[12] F. Honhang, L. Kachu, and S. Shukong, Jpn. J. Appl. Phys. **41**, L1122 (2002).
[13] V. I. Arkhipov *et al.*, J. Phys. Condens. Matter **14**, 9899 (2002).
[14] M. Koehler and I. Biaggio, Phys. Rev. B **68**, 075205 (2003).
[15] V. I. Arkhipov, P. Heremans, E. V. Emelianova, and H. Bassler, Phys. Rev. B **71**, 045214 (2005).
[16] J. L. Maldonado *et al.*, Chem. Mater. **15**, 994 (2003).
[17] D. V. Lang *et al.*, Phys. Rev. Lett. **93**, 086802 (2004).
[18] I. N. Hulea *et al.*, Phys. Rev. Lett. **93**, 166601 (2004).
[19] W. Gao and A. Kahn, J. Phys. Condens. Matter **15**, S2757 (2003).
[20] G. Horowitz, P. Lang, M. Mottaghi, and H. Aubin, Adv. Funct. Mater. **14**, 1069 (2004).
[21] L. Burgi, H. Sirringhaus, and R. H. Friend, Appl. Phys. Lett. **80**, 2913 (2002).
[22] G. Horowitz *et al.*, Adv. Mater. **10**, 923 (1998).
[23] O. Tal *et al.* (to be published).
[24] Ca. $V_{GS} - V_t \leq -3.5$ V and $V_{GS} - V_t \leq 15.6$ V for undoped and doped samples, respectively.
[25] G. Horowitz, R. Hajlaoui, and P. Delannoy, J. Phys. III **5**, 355 (1995).
[26] $V_t = 0.1 \pm 0.1$ V and $V_t = 0.8 \pm 0.1$ V as extracted from current-voltage curves taken on the undoped and doped OTFTs, respectively, according to Ref. [20].
[27] E. J. Meijer *et al.*, J. Appl. Phys. **93**, 4831 (2003).
[28] V. I. Arkhipov, E. V. Emelianova, and G. J. Adriaenssens, Phys. Rev. B **63**, 081202(R) (2001).